2021 27th International Conference on Mechatronics and Machine Vision in Practice (M2VIP) | 978-1-6654-3153-8/21/$31.00 ©2021 IEEE | DOI: 10.1109/M2VIP49856.2021.9664995

Untethered Cable-driven Soft Actuators for Quadruped Robots

Shoulu Gong, Jiahao Wu, Tianxiang Zheng, Wen-Ming Zhang, Lei Shao.

***Abstract*— Various soft robots have appealing advantages in human-machine interaction and industrial applications due to their intrinsic softness. However, the highly nonlinear response of soft material deformation makes the soft robotic system difficult to model and control. Recent attempts of kinematic modeling and control of soft robots mostly rely on simplified kinematic analysis or machine learning which are not accurate to guild their design and control. This work presents a cable driven untethered soft pneumatic actuator with its chambers inflated and sealed at all time. Its motion, including bending and stretching, can be well controlled by adjusting the cable length, and as a result, repeatable motions could be achieved and an accurate kinematic model can be also established. Based on our design, two untethered soft quadruped robots, one crawling and the other walking, are demonstrated for well-controlled forward and steering motions, which is indispensable toward soft robot control, cooperative operation and intelligent movement.**

I. INTRODUCTION

Soft robots have attracted great attention due to their excellent biocompatibility and potential applications in rescue, exploration, human-machine interaction and so on [1,2,3]. Soft robots are commonly made of soft materials (silicone rubber, etc.) or smart materials (liquid crystal elastomer, dielectric elastomers and shape memory polymer, etc.) and generally actuated by pneumatic, thermal and electrical signals. Compared to traditional rigid robots, soft robots usually have the characteristics of lightweight, infinite degree of freedom and mechanical compliance [4,5].

Various designs and actuation modes have been explored for soft robots, which endows them many application scenarios including crawling robots, quadruped robots and swimming robots, etc. Most soft robots are inspired by the movement of natural creatures [6], for instance, leveraging the elastic instabilities of pneumatic soft actuators to mimic the movement of cheetahs [7], using dielectric elastomers to fabricate electronic fish [8], and designing a phototactic self-sustained hydrogel oscillator based on photo thermal effect [9], among other various biomimetic robots [10,11,12] such as soft insect robot [13], soft jellyfish robot [14], etc.

However, there are two key challenges in soft robotics research still unresolved. First, soft robots often lack the ability to operate independently and must rely on external equipment (air pump, high-voltage power, etc.) for energy supply during the movement, which greatly constrains the deployment of soft robots. By contrast, untethered soft robots will not be restricted during their movement and have greater advantages in exploration. Lots of research effort on untethered soft robots has been done. The first pneumatic untethered soft robot was designed by Tolley et al. with an integrated battery for power supply [15], and later, an entirely soft and untethered robot was shown by Wehner et al. which was fabricated by 3D printing and driven by microfluidic chemical reactions without any electronics [16]. In addition, untethered soft flying robots powered by solar energy [17], untethered soft jellyfish robots actuated by magnetic field [18] and the pre-charged pneumatic untethered soft actuators [19] have been explored, too. However, there is still a lot of room for improvement towards the design of untethered soft robots for better actuation efficiency and more complicated deploying environment.

The other challenge lies in the kinematic modeling for soft robots because the highly nonlinear and unpredictable response of soft materials creates a huge difficulty to accurately analyze their dynamic behaviors. It also makes it difficult to achieve precise feedback control of soft robotic movements. To overcome this challenge, Patterson et al. used an external camera system to record the position of soft robots and realized navigation [20]. Thuruthel et al. reduced the motion error and achieved soft actuator perception based on embedded flexible sensors and recurrent neural networks [21，22]. There are other research efforts for modeling of soft robotic kinematics based on numerical analysis, such as absolute nodal coordinate formulation (ANCF) [23], and piecewise constant curvature method [24], but they are usually over-simplified to capture the real kinematics. Therefore, there lacks exploration by fundamentally redesigning the structure and actuation mechanisms of soft robots to minimize the influence of nonlinear material deformation.

In this work, we propose a novel untethered soft actuator with a controlled motion response and an accurate kinematic model, and also demonstrate its applications for soft quadruped robots including crawling and walking. Compared to traditional pneumatic soft actuators, this actuator is pre-inflated with a check valve sealing and driven by cables which are pulled or released using a motor. The bending angle of this soft actuator can be thus precisely calculated from the changing length of the cables, which eliminates the

*Research supported by the Shanghai Sailing Program of Shanghai Science and Technology Committee, China (Grant No. 19YF1425000), and the National Science Fund for Young Scientists of China (Grant No. 12002201).

Shoulu Gong is with the University of Michigan–Shanghai Jiao Tong University Joint Institute, Shanghai Jiao Tong University, Shanghai, China 200240 (e-mail: shoulu.gong@sjtu.edu.cn).

Jiahao Wu is with the University of Michigan–Shanghai Jiao Tong University Joint Institute, Shanghai Jiao Tong University, Shanghai, China 200240 (e-mail: wjh981123@sjtu.edu.cn).

Tianxiang Zheng is with the University of Michigan–Shanghai Jiao Tong University Joint Institute, Shanghai Jiao Tong University, Shanghai, China 200240 (e-mail: tianxiang.zheng@sjtu.edu.cn).

Wen-Ming Zhang is with the School of Mechanical Engineering and the State Key Laboratory of Mechanical System and Vibration, Shanghai Jiao Tong University, Shanghai, China 200240 (e-mail: wenmingz@sjtu.edu.cn).

Lei Shao is with the University of Michigan–Shanghai Jiao Tong University Joint Institute, Shanghai Jiao Tong University, Shanghai, China 200240 (corresponding author, phone: +86-21-34206567-5421; fax: +86-21-34206545, e-mail: lei.shao@sjtu.edu.cn).

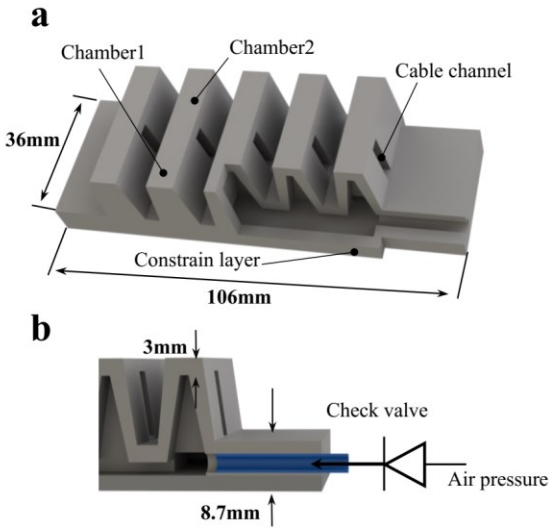

Figure 1. The prototype design of an inflated and sealed soft actuator. (a) The structure of the chambers and cable channels inside this soft actuator. (b) The design of an assembeled check valve for on-way sealing.

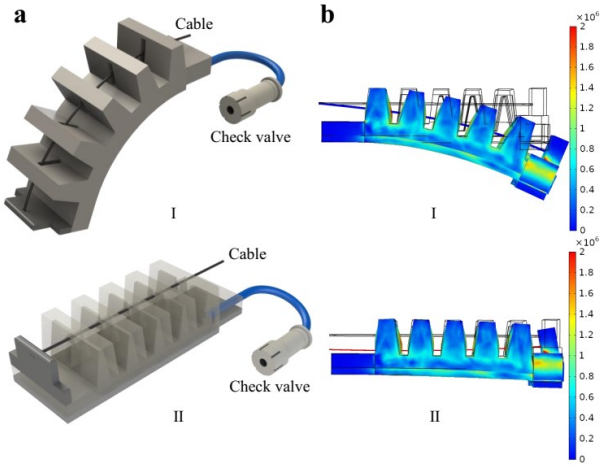

Figure 2. Actuation modes and finite element simulation. (a) The soft actuator is restored from the bending state to the initial state by pulling the cable. (c) The finite element simulation results of the same actuator in the two different states.

problematic nonlinear response between pressure and deformation in motion analysis and endows the soft actuator an accurate kinematic model. Based on this strategy, the actuator is shown experimentally to achieve a high repeatability between the input cable length and the output bending angle. Meanwhile, three motion modes can be easily realized, including a bending mode, a neutral mode and a reversed bending mode. We then show two untethered soft quadruped robots using these actuators as building blocks. One is a crawling robot which can achieve both forward and steering locomotions and can be well-controlled to complete a movement spanning an accurate distance. The other is a walking robot which can lift its legs to overcome hurdles and has the potential deployment in uneven and complex environment.

II. Design of the Untethered Soft Actuator

A. Structure and fabrication

Fig. 1a shows the structure of our soft actuator. The design is based on a common pneumatic actuator, where the upper layer is the bending layer and the bottom layer is the constrain layer. The actuator (the length is 106mm, the width is 36mm, the thickness is 8.7mm and the wall thickness of chamber is 3mm) has two separate chambers and a wide channel for cables, which ensures the free movement of the cables during bending. The chambers will expand with an applied air pressure, which makes the bending layer to stretch. The different amount of stretching between the bending layer and bottom layer leads to the bending of the actuator.

The check valve is used to seal and maintain air inside the chambers (Fig. 1b), with glue to bond the valve and the soft actuator to ensure air tightness. This soft actuator is manufactured by a single casting process, as the bending layer and the constrain layer are fabricated separately and then bonded together for simplified manufacturing process. The moulds are 3D printed by stereolithograhy using resin, while silicone rubber with hardness of 60A and 30A is used as the materials for the bending layer and the constrain layer, respectively.

B. Simulation and experimental measurement

Fig. 2a shows the working principle of the soft actuator. A non-stretchable cable was threaded through the channel and had its end fixed at the tip of the actuator with the other end wound to the steering wheel of a motor. When an air pressure is applied, the soft actuator will be inflated to bend towards the constrain layer and maintain such a bending state due to the presence of the check valve, which eliminates the need of external large pnematic equipments such as air pumps. It can then return to the neutral state (inflated with cable pulling) from the bending state (inflated with no cable pulling) by pulling the cable, and the soft actuator can also maintain at any bending angle by keeping the length of cable at constant as well. Fig. 2b shows the finite-element simulation of this soft actuator in a bending state and a neutral state which returns to a straight shape same as before inflation. We note that there is no squeezing between neighboring chambers and nor air leakage during all of these deformation processes.

Because the bending angle of this actuator is controlled by pulling or releasing the cables instead of controlling the pressure using a pump, we can easily integrate small motors, batteries and control boards onto it to eliminate any tethered wires, pumps or hoses. Such an untethered design enables this soft actuator to operate independently without being restricted by wired energy sources and greatly broadens it application scenarios.

Furthermore, traditional pneumatic soft actuators are difficult to model and control due to the nonlinear and unrepeatable relationship between pressure and bending angle. In contrast, the proposed actuator in this work relies on controlling by cable pulling or releasing. Thus, its kinematic model can be derived based on the direct geometric relationship between the changing length of the cable and the bending angle, which is much more accurate than controlling

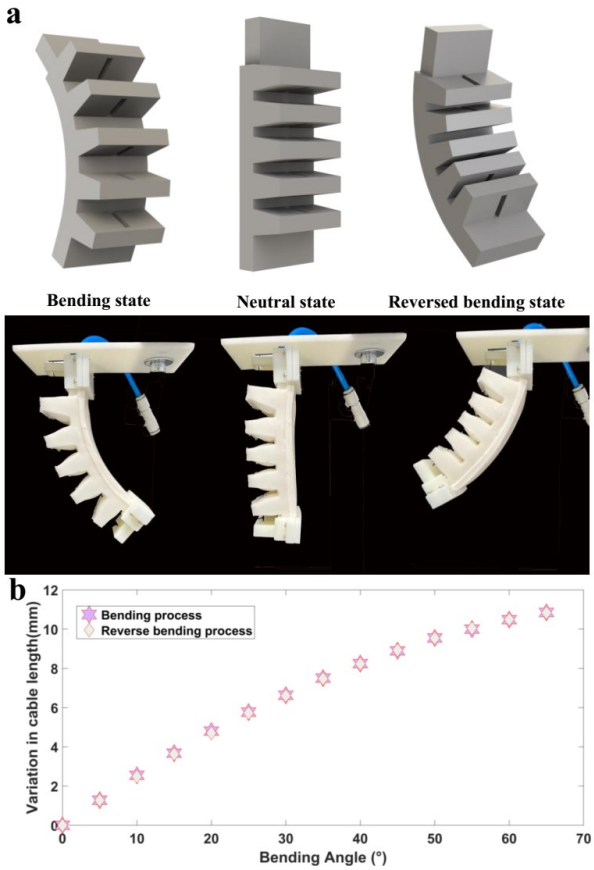

Figure 3. Motion states and kinematic test. (a) Three motion states of the cable-driven inflated and sealed actuator, including a bending state, a neutral state and a reversed bending state. (b) The relationship between the change in cable length and the bending angle shows excellent repeatability between the forward bending motion and reversed beding motion.

angle by varying pressure. This could potentially enable precise and repeatable motion control of our actuators.

Similar as other pneumatic soft actuators, this cable-driven soft actuator can also achieve three motion states including a bending state with a range of angles, a neutral state with a zero-degree angle and a reversed bending state with a range of negative angles (as shown in Fig. 3a). Therefore, this cable-driven actuation design enables the ability of bidirectional movement, which ensures great potential in untethered complex locomotion operation by assembling several of these actuators into various robots.

In addition, an experiment was conducted to test the accuracy and repeatability of its motion, as shown in Fig. 3b. For this experiment, the actuator was first inflated and sealed and was then pulled back to its neutral state, followed by a measurement of the actuator angle as a function of the changing cable length during the bending process and the reversed bending process. The cable length was varied as the motor rotated and the bending angle was obtained by processing the images of the actuator taken by a camera. The testing result shows excellent repeatability for forward motion and reversed motion with no hysteresis between the output bending angle and the input cable length. The achieved

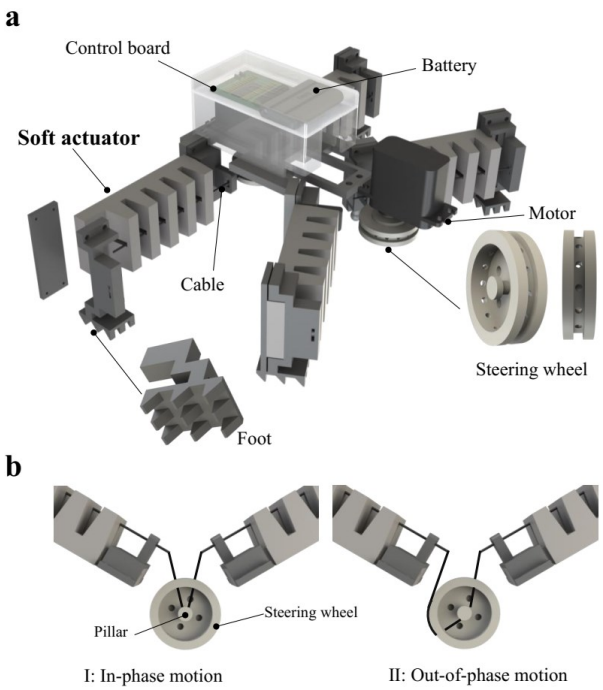

Figure 4. Design and actuation principle of an untethered soft crawling robot. (a) Structure and key components, including the control and power module, four actuation legs and their connections to the body, design of the steeering wheel and the feet. (b) Two winding types delivering 1) in-phase motion, for which one motor simultaneously drives the two actuators to undergo the same movement, and 2) out-of-phase motion, for which one motor simultaneously drives the two actuators to undergo opposite movements.

repeatability is much better than those actuators with the varying air pressure as their input.

III. UNTETHERED SOFT CRAWLING ROBOTS

A. Design

Soft robots have great potential in human-machine interaction and environment exploration due to the excellent softness and biocompatibility. Untethered soft crawling robots based on this soft actuator can achieve omnidirectional locomotion (both translational and steering motions), and the feature of accurate model and control could greatly improve the motion accuracy. Fig. 4a shows the prototype of such an untethered soft crawling robot, which contains four soft actuators as the building blocks assembled to a body carrying a control board, a battery and two motors. At the tip of each soft actuator, a spiked foot was attached to provide support and friction with the ground. The four soft actuators were first inflated and sealed, and then connected to the body. As shown in the previous section, the motors could potentially achieve precise control of the soft actuator by controlling the length of the cables.

In this design, one motor was used to control two adjacent soft actuators, while the cables threaded inside the channels were wound to the motors through a steering wheel. The connection between the cables and the motor determines the synchronous motion of the two soft actuators driven by the same motor, which is achieved by specially designed cable

winding at the steering wheel. Around the edge of this wheel, there are many equal-spaced small holes inside its groove (Fig. 4a), which are used for the cables to thread through. The cable first threads through a hole, then is wound to the pillar in the center of the steering wheel and finally exits the wheel through another hole. Fig. 4b shows two types of connection, one an in-phase arragenment for which the two actuators always moving in the same direction and the other out-of-phase for opposite directions. First, for the in-phase motion of the two actuators, the cable threaded through two actuators with the steering wheel in between symmetrically, and as a result, both soft actuators undergo the same motion state regardless of the rotational direction of the motor because of the same cable lengths in the two actuators maintaind at all time. For the other out-of-phase arragenment between the two actuators, the cable threaded through the steering wheel asymmetrically so that the length in one actuator at initial state is maximized and the other minimized. Therefore, the cable is pulled in one actuator while the other released as the motor rotates, and thus the two actuators undergo an opposite motion state. For both scenarios,

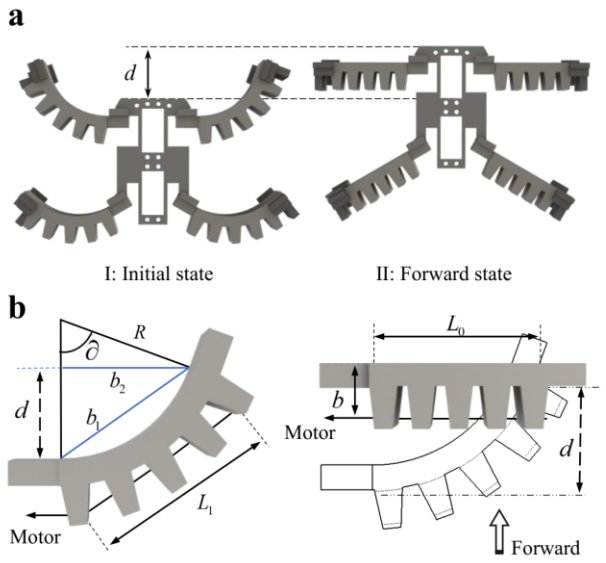

Figure 5. The kinematic model of the untethered soft crawling robot. (a) A four-legged crawling schematic mimicing the locomotion of sea turtles. (b) The kinematic model of one actuator as the motor pulling cables torwards the left side and the feet underneath the right end staying undisplaced during its motion cycle.

the motor rotation angle and frequency determine the motion amplitude and frequency of the actuators, respectively.

B. Kinematic model of untethered soft crawling robots

Fig. 5a shows the turtle-like motion of this crawling robot, for which the front and rear actuators have the same motion state. Initially, all four actuators are bent before the motor pulling the cables. After the motors are turned on by the control board, all four actuators are pulled to a straight shape (neutral state). The forward motion is realized by exploring the different frictional force between forward and backward motions due to the foot microstructures. Thus, the four feet stay at their position and push the body forward by a displacement of *d*. Then, the motors release the cables so the actuators bend again, resulting the robot stretching the feet forward and waiting for the next pulling action from the motors. The robot crawls forward if this cycle is kept on.

Compared to the nonlinear and poorly-characterized relationship between air pressure and bending angle for traditional pneumatic soft actuators, the untethered soft actuator in this work can establish an accurate kinematic model since the actuation is dependent on the cable length instead of pressure, so as the crawling robot. Such a design has great benefit in realizing an accurate motion feedback and control, leading to a well controlled locomotion.

As shown in Fig. 5b, the initial state of the actuator is under a bending state, and when the motor pulls the cable, the actuator returns to the neutral state, pushing the left-side tip of the actuator forward while the right side, with the foot underneath, is stuck with no motion due to friction with respect to ground. For this actuator, the bending angle is ∂ and the tip displacement is d during one motion cycle. Under the neutral state, the length of both the cable and the constrain layer is L_0, and the distance between the cable and the constrain layer is b. And when the bending angle of the actuator is ∂, the length of the cable is L_1, the radius of curvature is R. Thus, we can derive their relationship using simple geometry as below.

$$R=\frac{L_0}{\partial} \tag{1}$$

$$L_1 = 2(R+b)\sin\frac{\partial}{2} \tag{2}$$

$$\Delta L=2(R+b)\sin\frac{\partial}{2}-L_0 \tag{3}$$

When the cable drives the actuator moving from the bending state to the neutral state, the change in angle is ∂, and the displacement of the left tip in the forward direction is d. b_1 and b_2 are the side lengths of the right triangle shown in Fig. 5b. Therefore, the relationship can be derived as below:

$$b_1 = 2\cdot\frac{L_0}{\partial}\cdot\sin\frac{\partial}{2} \tag{4}$$

$$b_2 = \frac{L_0}{\partial}\cdot\cos\partial \tag{5}$$

$$d=\sqrt{4\cdot(\frac{L_0}{\partial}\cdot\sin\frac{\partial}{2})^2-(\frac{L_0}{\partial})^2\cdot\cos^2\partial} \tag{6}$$

It is clear that the angles and locomotion displacement are not depedent on pressure but simple geometry. As a result, an accurate kinematic model of this untethered soft crawling robot is established based on the cable-driven soft actuators.

C. Forward and steering motions

The crawling robot shows the ability to respond to specific locomotion instructions, and can achieve controlled movement based on the accurate kinematic model. Fig. 6a shows that it responded to a control command and moved a specific distance following a straight line. This was achieved by using the in-phase winding arragement at the steering wheels (Fig. 4b).

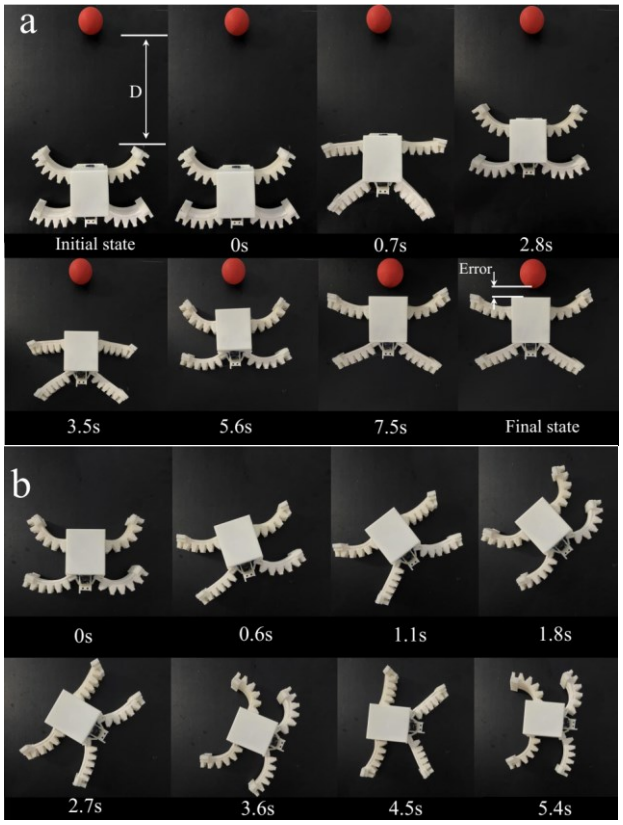

Figure 6. Demonstrations of forward and steering motions for the untethered soft crawling robot. (a) Forward tranalational motion spanning a certain distance *D* with calculated motor angle and cycling number, leading to a small error in the end. (b) Steering in-plane motion finising a 83-degree turning within 5.4 seconds.

Here, the initial distance between the robot and the target object is *D*, and the motion period is aboout 1.4 s. This crawling robot can reach the specific position after the pre-calculated number of cycles based on known relationship between motor rotational angle and robot displacement in one motion cycle. The crawling speed is about 37.4 mm/s.

There is a slight position error between the target position and the real final positon during experiments. This error is most likely due to slipping between the soft robot feet and the contact surface. The error can be significantly reduced by increasing contact friction or increasing load, which also demonstrates the capability of carrying payload while performing exploration and other tasks. In addition, this robot can also achieve steering motions. As shown in Fig. 6b, the untethered soft robot completed a steering motion as the two actuators controlled by the same motor performed asymmetric motions by using the out-of-phase winding arragement shown in Fig. 4b. The turning angle of this crawling robot is about 83 degrees which happened in 5.4 seconds.

IV. Untethered Soft Walking Robot

A. Design

The cable-driven actuator in this work can also be used to build an untethered walking quadruped robot. As shown in Fig. 7a, this robot is consisting of four actuators assembled upright to the body, two motors, one control board and one battery.

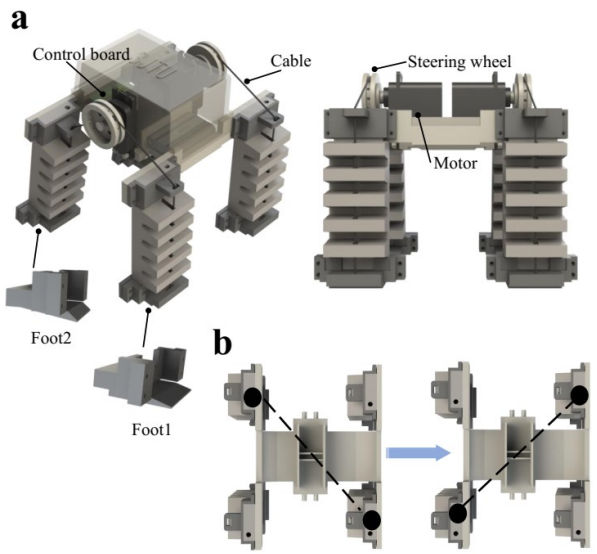

Figure 7. The design of an untethered soft quadruped robot. (a) Overall design with key components labeled. (b) Skematic diagram of the moion sequence showing the diagonal feet undergo the same motion simultaneously.

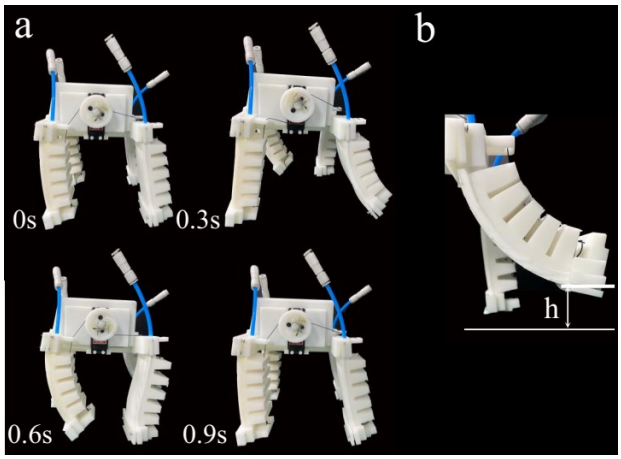

Figure 8. Demonstration of the quadruped walking robot. (a) The four steps involded in one motion cycle as the robot is walking to the right side. (b) The height of the foot off the ground, which can be benefial for overcoming hurdles during exploration.

Underneath each actuator, different kinds of foot were designed to ensure steady and efficient motion. All parts are manufactured by 3D printing using stereolithographic resin. All actuators are pre-inflated and sealed, and the initial bending state can be adjusted by controlling the cable length, which can be easily done using a motor. According to the same spirit of the crawling robot, one motor is used to control two actuators on the same side through a steering wheel. Fig. 7b shows the motion sequence of this quadruped robot. The two actuators controlled by the same motor move in the opposite directions, and as a result, the two diagonal actuators have the same motion state, similar as some quadruped animals.

B. Experiments

Fig. 8a shows the forward motion of the soft quadruped robot, as the actuators switching between the bending state and the reversed bending state by controlling the cable length. One complete motion cycle includes four steps, which corresponds to the different gestures of four legs. This process involves a set of diagonal legs lifting up and then pushing the ground to move its body forward, followed by the other set of diagonal legs performing the same motion. The reversed bending state of the soft actuators corresponds to the motion lifting legs, while the bending state of the soft actuators corresponds to the motion pushing ground and move forward its body center of mass.

Finally, as shown in Fig. 8b, the height of the feet, *h*, as the robot lifting its feet, is directly related to the length of cable pulling. Based on this design, the robot is also able to overcome certain hurdles lower than a height of *h*.

V. Conclusion

In this paper, we proposed a novel untethered soft actuator as one solution to overcome the challenge that most soft actuators depend on tethered external equipment. This is achieved by pre-inflation and sealing of the pneumatic soft body combined with cable actuation. More important, an accurate kinematic model can be established because the actuator bending angle is solely dependent on the well-controlled cable length instead of varying air pressure which is commonly used for conventional pneumatic actuators. This actuator has three motion states, including bending state, neutral state and reversed bending state, depending on the cable length, which endows the soft actuator a larger motion range and more application scenarios. We also demonstrate the application of this soft actuator in untethered soft robots, including a crawling robot and a walking robot. The untethered soft crawling robot can achieve both forward and steering motions with an accurate kinematic model, as it can exactly move a pre-calculated distance. And on the other hand, the untethered soft walking robot mimics the movement of a quadruped animal and can step over certain obstacles.

For the work mentioned in this article, there is still room for optimization of the two types of untethered soft robots to ensure accuracy and robustness. For example, the foot structure can be redesigned to minimize slipping with ground during movement. In addition, closed-loop control can be achieved with the help of external sensing equipment such as a camera system. For the future follow-up work, we will expand the application scenarios based on this soft actuator to realize navigation, cluster control, and also feedback control based on the accurate kinematic model as well.

References

[1] S. Kim, C. Laschi, and B. Trimmer, "Soft robotics: a bioinspired evolution in robotics," *Trends in Biotechnology*, vol. 31, no. 5, pp. 287–294, 2013.

[2] D. Rus and M. T. Tolley, "Design, fabrication and control of soft robots," *Nature*, vol. 521, no. 7553, pp. 467–475, 2015.

[3] S. Chen, Y. Cao, M. Sarparast, H. Yuan, L. Dong, X. Tan, and C. Cao, "Soft Crawling Robots: Design, Actuation, and Locomotion," *Advanced Materials Technologies*, vol. 5, no. 2, p. 1900837, 2019.

[4] S. I. Rich, R. J. Wood, and C. Majidi, "Untethered soft robotics," *Nature Electronics*, vol. 1, no. 2, pp. 102–112, 2018.

[5] M. Cianchetti, C. Laschi, A. Menciassi, and P. Dario, "Biomedical applications of soft robotics," *Nature Reviews Materials*, vol. 3, no. 6, pp. 143–153, 2018.

[6] X. Y. Guo, W. B. Li, and W. M. Zhang, "Adjustable stiffness elastic composite soft actuator for fast-moving robots," *Science China Technological Sciences*, 2021.

[7] Y. Tang, Y. Chi, J. Sun, T.-H. Huang, O. H. Maghsoudi, A. Spence, J. Zhao, H. Su, and J. Yin, "Leveraging elastic instabilities for amplified performance: Spine-inspired high-speed and high-force soft robots," *Science Advances*, vol. 6, no. 19, 2020.

[8] T. Li, G. Li, Y. Liang, T. Cheng, J. Dai, X. Yang, B. Liu, Z. Zeng, Z. Huang, Y. Luo, T. Xie, and W. Yang, "Fast-moving soft electronic fish," *Science Advances*, vol. 3, no. 4, 2017.

[9] Y. Zhao, C. Xuan, X. Qian, Y. Alsaid, M. Hua, L. Jin, and X. He, "Soft phototactic swimmer based on self-sustained hydrogel oscillator," *Science Robotics*, vol. 4, no. 33, 2019.

[10] D. S. Shah, J. P. Powers, L. G. Tilton, S. Kriegman, J. Bongard, and R. Kramer-Bottiglio, "A soft robot that adapts to environments through shape change," *Nature Machine Intelligence*, vol. 3, no. 1, pp. 51–59, 2020.

[11] A. Joshi, A. Kulkarni, and Y. Tadesse, "FludoJelly: Experimental Study on Jellyfish-Like Soft Robot Enabled by Soft Pneumatic Composite (SPC)," *Robotics,* vol. 8, no. 3, p. 56, 2019.

[12] D. Xie, J. Liu, R. Kang, and S. Zuo, "Fully 3D-Printed Modular Pipe-Climbing Robot," *IEEE Robotics and Automation Letters*, vol. 6, no. 2, pp. 462–469, 2021.

[13] Y. Chen, H. Zhao, J. Mao, P. Chirarattananon, E. F. Helbling, N.-seung P. Hyun, D. R. Clarke, and R. J. Wood, "Controlled flight of a microrobot powered by soft artificial muscles," *Nature*, vol. 575, no. 7782, pp. 324–329, 2019.

[14] Z. Ren, W. Hu, X. Dong, and M. Sitti, "Multi-functional soft-bodied jellyfish-like swimming," *Nature Communications*, vol. 10, no. 1, 2019.

[15] M. T. Tolley, R. F. Shepherd, B. Mosadegh, K. C. Galloway, M. Wehner, M. Karpelson, R. J. Wood, and G. M. Whitesides, "A Resilient, Untethered Soft Robot," *Soft Robotics*, vol. 1, no. 3, pp. 213–223, 2014.

[16] M. Wehner, R. L. Truby, D. J. Fitzgerald, B. Mosadegh, G. M. Whitesides, J. A. Lewis, and R. J. Wood, "An integrated design and fabrication strategy for entirely soft, autonomous robots," *Nature*, vol. 536, no. 7617, pp. 451–455, 2016.

[17] N. T. Jafferis, E. F. Helbling, M. Karpelson, and R. J. Wood, "Untethered flight of an insect-sized flapping-wing microscale aerial vehicle," *Nature*, vol. 570, no. 7762, pp. 491–495, 2019.

[18] M. E. Sayed, J. O. Roberts, R. M. McKenzie, S. Aracri, A. Buchoux, and A. A. Stokes, "Limpet II: A Modular, Untethered Soft Robot," *Soft Robotics*, vol. 8, no. 3, pp. 319–339, 2021.

[19] Y. Li, Y. Chen, T. Ren, Y. Li, and S. hong Choi, "Precharged Pneumatic Soft Actuators and Their Applications to Untethered Soft Robots," *Soft Robotics*, vol. 5, no. 5, pp. 567–575, 2018.

[20] Z. J. Patterson, A. P. Sabelhaus, K. Chin, T. Hellebrekers, and C. Majidi, "An Untethered Brittle Star-Inspired Soft Robot for Closed-Loop Underwater Locomotion," *2020 IEEE/RSJ International Conference on Intelligent Robots and Systems (IROS)*, 2020.

[21] T. G. Thuruthel, B. Shih, C. Laschi, and M. T. Tolley, "Soft robot perception using embedded soft sensors and recurrent neural networks," *Science Robotics*, vol. 4, no. 26, 2019.

[22] B. Shih, D. Shah, J. Li, T. G. Thuruthel, Y.-L. Park, F. Iida, Z. Bao, R. Kramer-Bottiglio, and M. T. Tolley, "Electronic skins and machine learning for intelligent soft robots," *Science Robotics*, vol. 5, no. 41, 2020.

[23] X. Huang, J. Zou, and G. Gu, "Kinematic modeling and control of variable curvature soft continuum robots," *IEEE/ASME Transactions on Mechatronics*, pp. 1–1, 2021.

[24] P. Abbasi, M. A. Nekoui, M. Zareinejad, P. Abbasi, and Z. Azhang, "Position and Force Control of a Soft Pneumatic Actuator," *Soft Robotics*, vol. 7, no. 5, pp. 550–563, 2020.